

# AVOIDING COMBINATORIAL EXPLOSION IN SIMULATION OF MULTIPLE MAGNET ERRORS IN SWAP-OUT SAFETY TRACKING FOR THE ADVANCED PHOTON SOURCE UPGRADE\*

M. Borland, R. Soliday, ANL, Argonne, IL 60439, USA

## Abstract

The Advanced Photon Source (APS) is upgrading the storage ring to provide a natural emittance of 41 pm at 6 GeV. The small dynamic acceptance entails operation in on-axis swap-out mode. Careful consideration is required of the safety implications of injection with shutters open. Tracking studies require simulation of multiple simultaneous magnet errors, some combinations of which may introduce potentially dangerous conditions. A naive grid scan of possible errors would be prohibitively time-consuming. We describe a different approach using biased sampling of particle distributions from successive scans.

## INTRODUCTION

A large bending-magnet error in a light source ring could allow injected-beam electrons to enter a photon beamline, perhaps resulting in beam exiting the tunnel. Similarly, such a failure could allow injected beam to hit structures near or within the front end, producing a potentially hazardous radiation shower down the beamline. One safeguard is to disallow injection with shutters open if there is no stored beam present [1], since stored beam is very unlikely if there is magnet error that is sufficiently large to allow hazardous endpoints for injected beam. Depending on the regulatory environment, this assertion may be considered sufficient or may need support from simulations [1–6]. In some cases [2, 4, 5, 7], the stored beam interlock was found insufficient, though this may be a result of conservative assumptions.

Simulation strategies include forward tracking of the potential injected beam phase space or backward tracking of the hypothetical phase space of hazardous particles. The latter is less beneficial when considering a radiation shower generated by beam striking components at the entrance of the photon beamline or in the front end. Since this is a concern for APS-U [8, 9], which will operate in swap-out mode [10, 11], we have used forward tracking [12].

The present paper deals with the issue of multiple magnet errors in a multi-bend achromat lattice [13] with many independently-powered dipoles [8]. Our simulations use elegant [14, 15] to track through computed 3D field maps that extend over the photon channels, which reduces the need for approximations and assumptions in treating the character of the fields outside the good field region, including areas outside the magnet. Physical apertures and multiply-connected vacuum chambers are defined using midplane

boundaries around “no-go” regions, which allows very rapid determination of particle strikes using winding number computations [12].

## SIMULATING MULTIPLE SIMULTANEOUS ERRORS

Previously [12], we simulated the effects of single magnet errors, which is manageable even with 10’s of millions of simulation particles and using relatively small (2%) steps in the error. The preliminary conclusion was that concerns exist, but typically for large magnet errors that are incompatible with stored beam.

However, nothing prevents faults in or adjustments to multiple magnets. For example, for a bending-magnet (BM) beamline, we consider eight magnets, designated A:Q7, A:M3, A:Q8, A:M4, B:Q8, B:M3, B:Q7, and B:M2. In single-magnet studies, only the A:M4, B:Q8, and B:M3 can steer particles to dangerous endpoints. To this list, we added consideration of three upstream magnets (A:Q7, A:M3, A:Q8) and two downstream magnets (B:Q7, B:M2). All except B:M2 have two power supplies: a main supply that varies the dipole and quadrupole field and a trim supply that varies only the dipole.

We plan to use software monitoring to prevent the current in any magnet from deviating by more than, say, 10% from its nominal setpoint. While we might naively imagine scanning each magnet over  $\pm 10\%$  with a step size of 2%, this requires  $11^{15} \approx 4 \times 10^{15}$  runs. In this naive concept, each run has specific errors in each magnet, but takes beam from the beginning to the end of the sector; we combine many runs to understand the landscape. An alternative approach involves tracking the beam through each magnet in turn, scanning as we go, with the beam building up the effect of the previous scans [6]. Except for the first run, each run includes only one magnet plus some downstream drift spaces. While the workload is reduced, the problem is still unmanageable since the number of particles increases dramatically after each element. To address this, we observe that many particles are close to other particles in  $(x, x', y, y', \delta)$  phase space, and give redundant information. If we down-sample by a factor equal to the number of scan points in a single run, the workload is constant.

## DOWN-SAMPLING

For a 31 x 31 grid scan of each magnet’s main and trim supplies, we should down-sample  $\sim 1000$ -fold. If tracking is limited to  $(x, x')$ , phase-space repopulation [6] can be used to create a new distribution, but this is problematic in five dimensions. Assuming constant phase-space density,

\* Work supported by the U.S. Department of Energy, Office of Science, Office of Basic Energy Sciences, under Contract No. DE-AC02-06CH11357.

we could generate a uniform random deviate  $U_i : [0, 1]$  for each particle and retain only particles with  $U_i \leq 1/1000$ . Though reasonable, this purely random sampling may undersample unusual or outlying particles that are more likely to be problematic.

Biased downsampling, which preferentially retains particles in low-density regions, is superior. We use kernel density estimation (KDE) [16] to determine for each particle a density value based on the proximity of other points in phase space. The code, `sddslocaldensity`, is part of the SDDS Toolkit [17, 18] and is parallelized using OpenMP.

The ideal selection algorithm would produce a particle distribution with constant density in five dimensional phase space, but this is not essential and would be difficult to achieve. After some experimentation, we devised a selection method that is a simple modification of the uniform random method. Let  $P_i$  represent the local density at the location of the  $i^{th}$  particle, with  $P_u$  and  $P_l$  giving the maximum and minimum values, respectively. For each particle, we compute the normalized density  $Q_i = P_i/P_u$ , which ranges between  $P_l/P_u \approx 0$  and 1. We define a selection threshold for each particle as  $T_i = \beta + (\alpha - \beta)(1 - Q_i)^\gamma$ , where  $0 \leq \alpha \leq 1$ ,  $0 \leq \beta \leq \alpha$ , and  $\gamma > 0$  are quantities we tune to get the desired selection. We keep those particles for which  $U_i < T_i$ .  $\alpha$  ( $\beta$ ) is the selection probability for particles in low-density (high-density) regions.

Since down-selection in five dimensions is hard to visualize, for illustration we took the 1.4-billion-particle beam from a  $31 \times 31$  scan of A:Q7 and performed KDE using the  $x$  and  $\delta = \Delta p/p_0$  coordinates. Since we want to down-sample by a factor of  $\sim 1000$  overall, we need  $\beta \sim 10^{-3}$ . Through various trials, we found that using  $\alpha = 5\beta$  and  $\gamma = 2$  works well. Particles in low-density regions are about five times as likely to be selected as those in high-density regions. Using smaller  $\beta$  and larger  $\alpha$  may result in a “hollow” beam that lacks representation in high density areas. As Figs. 1 and 2 show, the downsampled particle distribution is more uniform than the original distribution and preferentially samples the low-density region.

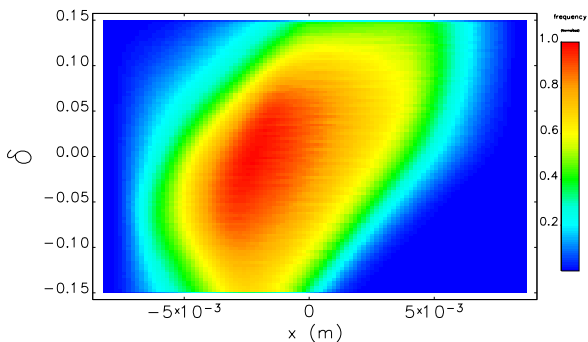


Figure 1: Distribution without down-selection.

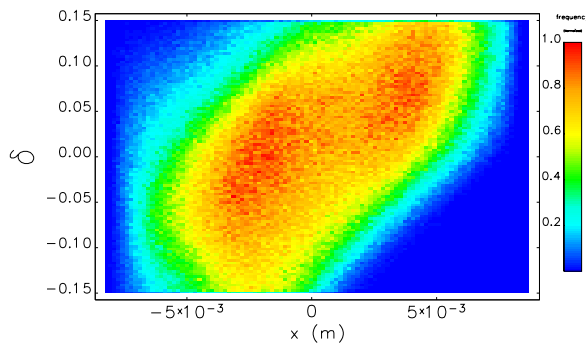


Figure 2: Distribution after biased down-selection.

## STRUCTURING THE RUNS

The approach of sweeping each magnet in turn as we work the beam down the beamline requires taking the beam from each “upstream” run and injecting it into the next “downstream” run at the point where the previous run ended. For a BM line, our first run would start at the center of the straight section and track through the first varied element, e.g., A:Q7, ending just before the next varied element A:M3. This can be accomplished without editing the lattice file using `elegant`’s `change_end` command. The second run would begin at the entrance to A:M3. Using the `change_start` command for this would complicate the global-coordinate definition of the apertures; instead, we use `insert_elements` to add a marker just before the next-varied element and also to insert a `BRANCH` command at the start of the beamline to jump to that marker. This preserves the floor coordinates while avoiding error-prone editing of lattice files.

To perform the runs, we created a series of command files that perform tracking with the variation of a single element, then ran them in the proper order. In between, we used the techniques just described to down-select the particles using 5D KDE. Each value of the main varied element was simulated in a separate run, producing a separate lost-particle file and output-particle file. Within each run, a `vary_element` loop is used to vary the trim, if any.

For the BM case, we scanned over  $\pm 30\%$ , fully expecting to find dangerous particles. Having encoded the indices of the grid into the `particleID` property in the lost-particle data files, we were able to analyze the number of dangerous particles as a function of the fractional strength error (FSE) limit for the main supplies. (Specifically, since we used 31 grid points for each scan, we used the scan indices, running from 0 to 30, as “digits” in base 31, which we carry in the particle ID.) As shown in Fig. 3, if the FSE is limited to  $\pm 12\%$ , no dangerous endpoints are predicted. We plan to use a fail-safe software-based monitor to enforce this limit.

## INSERTION DEVICE BEAMLINES

For the insertion device (ID) beamlines, we are concerned about a smaller set of magnets: three independently-powered quadrupoles (A:Q1, A:Q2, A:Q3), one string-

powered longitudinal-gradient dipole (A:M1), one horizontal corrector (A:FH1), and one independently-powered sextupole with a horizontal steering trim (A:S1, A:H1). While this is a less demanding problem than the BM beamlines, one complication is the need to simulate coil shorts in the string-powered A:M1 dipole [12]. To date, we've completed a pre-production run for this case, scanning the main supplies over  $\pm 10\%$  and the steering trims over their full range, including 15 shorting scenarios. We started with  $1.4 \times 10^7$  acceptance-filling particles and maintained about  $5 \times 10^7$  particles after down-selection.

Under these conditions and assuming an incoming beam energy range of  $\pm 9\%$ , only four shorting cases permit dangerous particles. These correspond to shorting of 9, 10, and 11 layers, plus a full short of a single coil. Simulations of stored beam show that nearby steering trims are sufficient to restore the existence of the closed orbit when accompanied by tune correction for the 9-layer short, but not the others. As Fig. 4 shows, we can restrict the range of errors (or adjustments) in the A:Q1, A:Q2, and A:Q3 to  $\pm 8\%$  and ensure that the case with 9 shorted layers does not produce any dangerous particles. Note that a short of only 9 layers in one coil is too small to be easily detected by the planned interlock on the power supply voltage [19].

Our analysis does not enforce consistency between the stored beam and escaping beam simulations. Rather, we conservatively assume that if, for the same A:M1 short, we can find conditions that allow both stored beam and escaping beam, then the potential for an accident is such that we must introduce a means of preventing the escaping beam case from being realized. One reason for making this assumption is that there are so many independent steering trims and quadrupoles. Another is to avoid having to evaluate the closed orbit for each of the many configurations that might generate dangerous particles.

## NEXT STEPS

The work so far emphasized development of techniques and performing pre-production runs. Production runs will utilize wider and finer scans, e.g.,  $\pm 30\%$  variation in main supplies with steps of 1%. It is important to use a wider range for the sextupole magnets, since significant adjustments may be desired as the lattice is empirically optimized.

APS-U lattice nonlinear dynamics optimization [20] uses many independently-powered sextupoles. So far, we've used the sextupole configuration for one sector tuned for the vertical-plane injection scheme [21]. For the new horizontal-plane injection scheme [22], there are four unique sector configurations, but only two are used in sectors with photon beamlines.

We will also use aperture data that is sliced at a vertical resolution of  $100 \mu\text{m}$ ; this removes a overly-conservative assumption about the vertical variation of the apertures and allows providing more useful data to downstream radiation transport computations.

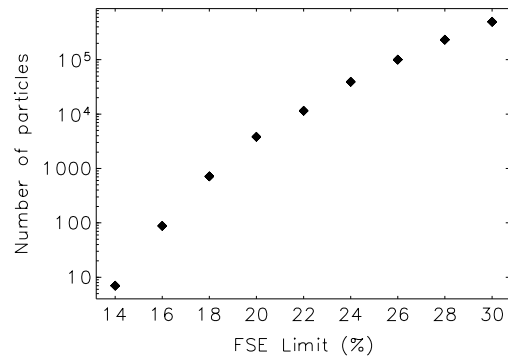


Figure 3: Number of “dangerous” particles predicted for BM beamline as a function of the limiting fractional strength error on relevant power supplies.

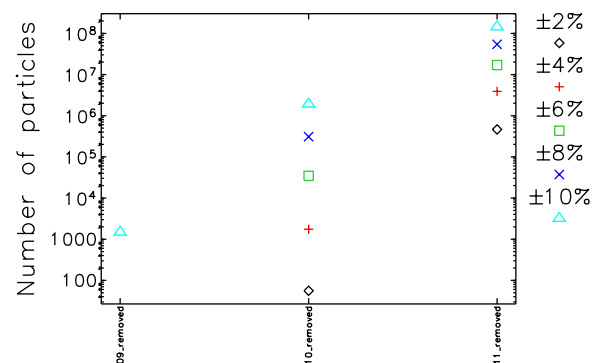


Figure 4: Remaining particles for various A:M1 shorting cases and limits on the fractional strength error of relevant quadrupoles, for full range of A:S1 steering supply.

## CONCLUSIONS

We have developed and applied a methodology for efficiently performing multi-dimensional scans of magnet strengths to assess safety issues for swap-out operation of the Advanced Photon Source Upgrade. The method relies on kernel density estimation in five dimensions to provide an estimate of the local phase-space density near each simulation particle; this allows down-sampling particle distributions to emphasize low-density areas, which contain more unique combinations of properties. This tames the combinatorial explosion inherent in a high-resolution, multi-dimensional scan. Pre-production runs for the insertion device and bending-magnet beamlines show that if main power supplies are kept within 8% and 12%, respectively, of their design setpoints, there is no indication that dangerous endpoints are reachable by injected beam. For the insertion device case, the stored-beam interlock comes into play by restricting the number of potentially concerning magnet-shortening cases.

## REFERENCES

- [1] L. Emery and M. Borland, “Analytical studies of top-up safety for the advanced photon source,” in *Proc. PAC’99*, New York, NY, USA, Mar. 1999, paper THA150, pp. 2939–2941.
- [2] M. Borland and L. Emery, “Tracking Studies of Top-Up Safety for the Advanced Photon Source,” in *Proc. PAC’99*, New York, NY, USA, Mar. 1999, paper WEP26, pp. 2319–2321.
- [3] I. P. S. Martin, C. P. Bailey, R. Bartolini, E. C. Longhi and R. P. Walker, “Top-Up Safety Simulations for the Diamond Storage Ring,” in *Proc. EPAC’08*, Genoa, Italy, Jun. 2008, paper WEPC044, pp. 2085–2087.
- [4] H. Nishimura *et al.*, “Advanced light source’s approach to ensure conditions for safe top-off operation,” *Nucl. Instrum. Methods Phys. Res., Sect. A*, vol. 608, no. 1, pp. 2–18, 2009. doi: 10.1016/j.nima.2009.05.196
- [5] X. Huang *et al.*, “Tracking Study for Top-off Safety Validation at SSRL,” Tech. Rep. SLAC-PUB-14399, SLAC, 2011.
- [6] Y. Li, L. Yang, and S. Krinsky, “Efficient cascaded parameter scan approach for studying top-off safety in storage rings,” *Phys. Rev. ST Accel. Beams*, vol. 14, p. 033501, 2011. doi: 10.1103/PhysRevSTAB.14.033501
- [7] S. M. Liuzzo, P. Berkvens, J. Chavanne, N. Cariminani, and L. Farvacque, “Tracking Studies for Safe Top-Up Injection at ESRF-EBS,” Low Emittance Ring Workshop, 2018.
- [8] M. Borland, T. G. Berenc, R. R. Lindberg, V. Sajaev and Y. P. Sun, “Lower Emittance Lattice for the Advanced Photon Source Upgrade Using Reverse Bending Magnets”, in *Proc. NAPAC’16*, Chicago, IL, USA, Oct. 2016, pp. 877–880. doi: 10.18429/JACoW-NAPAC2016-WEPOB01
- [9] B. Micklich, 2020. Private Communication.
- [10] R. Abela, W. Joho, P. Marchand, S. V. Milton and L. Z. Rivkin, “Design Considerations for a Swiss Light Source (SLS)”, in *Proc. EPAC’92*, Berlin, Germany, Mar. 1992, pp. 486–489.
- [11] L. Emery and M. Borland, “Possible Long-Term Improvements to the Advanced Photon Source”, in *Proc. PAC’03*, Portland, OR, USA, May 2003, paper TOPA014, pp. 256–258.
- [12] M. Borland, J. S. Downey and M. S. Jaski, “Swap-Out Safety Tracking for the Advanced Photon Source Upgrade”, in *Proc. IPAC’21*, Campinas, Brazil, May 2021, pp. 249–252. doi: 10.18429/JACoW-IPAC2021-MOPAB058
- [13] D. Einfeld and M. Plesko, “A modified qba optics for low emittance storage rings,” *Nucl. Instrum. Methods Phys. Res., Sect. A*, vol. 335, no. 3, pp. 402–416, 1993. doi: 10.1016/0168-9002(93)91224-B
- [14] M. Borland, “elegant: A Flexible SDDS-Compliant Code for Accelerator Simulation,” Tech. Rep. LS-287, Advanced Photon Source, September 2000.
- [15] Y. Wang and M. Borland, “Implementation and Performance of Parallelized Elegant”, in *Proc. PAC’07*, Albuquerque, NM, USA, Jun. 2007, paper THPAN095, pp. 3444–3446.
- [16] Multivariate kernel density estimation, [http://en.wikipedia.org/wiki/Multivariate\\_kernel\\_density\\_estimation](http://en.wikipedia.org/wiki/Multivariate_kernel_density_estimation). Accessed: 2021-12-22.
- [17] M. Borland, “Applications Toolkit for Accelerator Control and Analysis”, in *Proc. PAC’97*, Vancouver, Canada, May 1997, paper 6P020, pp. 2487–2489.
- [18] R. Soliday, M. Borland, L. Emery and H. Shang, “New Features in the SDDS Toolkit”, in *Proc. PAC’03*, Portland, OR, USA, May 2003, paper FPAG005, pp. 3473–3475.
- [19] F. Rafael, “Private communication,” 2022.
- [20] M. Borland, V. Sajaev, L. Emery and A. Xiao, “Multi-objective Direct Optimization of Dynamic Acceptance and Lifetime for Potential Upgrades of the Advanced Photon Source,” Tech. Rep. ANL/APS/LS-319, APS, 2010.
- [21] A. Xiao and M. Borland, “Transport Line Design and Injection Configuration Optimization for the Advanced Photon Source Upgrade”, in *Proc. IPAC’18*, Vancouver, Canada, Apr.-May 2018, pp. 1287–1289. doi: 10.18429/JACoW-IPAC2018-TUPMF017
- [22] J. Liu, M. Borland, T. K. Clute, J. S. Downey, M. S. Jaski and U. Wienands, “Mechanical Design of the Booster to Storage Ring Transfer (BTS) Line for APS Upgrade”, in *Proc. MEDSI’20*, Chicago, USA, Jul. 2021, p. 279. doi: 10.18429/JACoW-MEDSI2020-WEPB06